



Original article

Intelligent reactive power control of renewable integrated hybrid energy system model using static synchronous compensators and soft computing techniques

Pabitra Kumar Guchhait^a, Samrat Chakraborty^{b,*}, Debottam Mukherjee^c, Ramashis Banerjee^d

^a Department of Electrical Engineering, G. H. Raisoni College of Engineering and Management, Pune, Maharashtra 412207, India

^b Department of Electrical Engineering, National Institute of Technology Arunachal Pradesh, Jote, Arunachal Pradesh 791113, India

^c Department of Electrical Engineering, Indian Institute of Technology (BHU), Varanasi, Uttar Pradesh 221005, India

^d Department of Electrical Engineering, National Institute of Technology Silchar, Assam 788010, India

ARTICLE INFO

Article history:

Received 25 September 2021

Accepted 30 March 2022

Available online xxxx

Keywords:

Wind-diesel hybrid power system
Transient stability
Static synchronous compensator
PID with derivative filter controller
Soft computing

ABSTRACT

Modern power system faces a severe problem of instability largely due to inconsistent reactive power. It causes damage to the power grid within a few milliseconds. Therefore, proper management of reactive power under disturbing situations has a key role in its safe operation. Devices such as flexible alternating current transmission systems (FACTS) accurately manage the system's reactive power in accordance with the load demand. In this study, a new reactive power control strategy is employed for optimization of the reactive power along with the stability improvement of the system under different small perturbed conditions. Therefore, this study focuses on controlling the reactive power for an isolated wind-diesel hybrid power system model (WDHPSM) with the aid of a static synchronous compensator (STATCOM) together with the use of an integral minus proportional derivative (IPD) controller keeping a derivative-based filter (IPDF) as a secondary controller for better utilization of its purpose. The obtained results are compared when the no control strategy is applied in the model. Another comparison has been done between the multiple applied soft computing techniques (oppositional harmonic search, ant lion optimization, binary-coded genetic algorithm, and symbiosis organisms search) which optimize the parameters of the controller of WDHPSM.

© 2022 The Authors. Production and hosting by Elsevier B.V. on behalf of King Saud University. This is an open access article under the CC BY-NC-ND license (<http://creativecommons.org/licenses/by-nc-nd/4.0/>).

1. Introduction

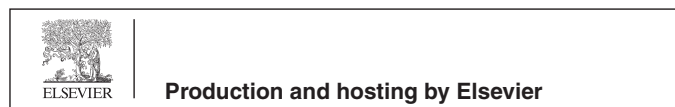
Over the last few years, researchers have been using various kinds of controllers, namely proportional (P), integral (I), and proportional-integral (PI) as secondary controllers for better ex-

Abbreviations: FACTS, Flexible alternating current transmission systems; WDHPSM, Wind-diesel hybrid power system model; STATCOM, Static synchronous compensator; ALO, Ant lion optimization; BGA, Binary-coded genetic algorithm; SOS, Symbiosis organism search; OHS, Oppositional harmonic search; SG, Synchronous generator; IG, Induction generator; IPDF, Integral minus proportional derivative filter; I-TD, Integral-tilt derivative; HM, Harmony memory.

* Corresponding author.

E-mail address: schaktu@gmail.com (S. Chakraborty).

Peer review under responsibility of King Saud University.



<https://doi.org/10.1016/j.jksues.2022.03.004>

1018-3639/© 2022 The Authors. Production and hosting by Elsevier B.V. on behalf of King Saud University.

This is an open access article under the CC BY-NC-ND license (<http://creativecommons.org/licenses/by-nc-nd/4.0/>).

Please cite this article as: Pabitra Kumar Guchhait, S. Chakraborty, D. Mukherjee et al., Intelligent reactive power control of renewable integrated hybrid energy system model using static synchronous compensators and soft computing techniques, Journal of King Saud University – Engineering Sciences, <https://doi.org/10.1016/j.jksues.2022.03.004>

with a filter in magnetic levitation systems as well as in frequency control in multi microgrid systems. The current study shows that I-TD is more suitable than TID controller. Rajinikanth and Latha (2012) reported that the I-PD controller is used for stability analysis of a single machine infinite bus (SMIB) system. The I-TD controller is analogous to the I-PD controller, only a tilt proportional term is added to the I-TD controller. Although various papers are presented taking TID, I-TD controller deployed for LFC of two area-integrated systems (Sain et al., 2016; Arya, 2019; Merrikh-Bayat, 2017; Sain et al., 2018; Morsali et al., 2018; Morsali et al., 2017), there is less focus on the reactive power control study using these controllers even though they are best performers than the other controllers in terms of their performance. This paper thus presents an I-PD with derivative filter (IPDF) controller merely as I-TD with derivative filter for reactive power control of a hybrid power system (HPS).

For obtaining a more stable performance of the HPS, the parameters of IPDF are tuned with meta-heuristic algorithms. In this work, ant lion optimization (ALO) (Ali et al., 2017), binary-coded genetic algorithm (BGA) (Kothari, 2012), symbiosis organisms search (SOS) (Hasanien and El-Fergany, 2016), and oppositional harmonic search (OHS) (Haridoss and Punniyakodi, 2019) algorithms are addressed to optimize the HPS parameters and to verify their effectiveness to the reactive power compensation. Therefore, this paper applied I-PD (with derivative filter) controller as a secondary controller associated with the static synchronous compensator (STATCOM) for reactive power flow studies of the considered wind-diesel HPS (WDHPS) model.

The reactive power requirement varies with the variable nature of wind power. Because of the limitations of excitation control, the synchronous generator (SG) may not dispense the requisite quantum of reactive power to the considered WDHPS. The deficit of reactive power will cause voltage fluctuations in the WDHPS model. Such deficit is not desirable in the system and is also sometimes not tolerable. Therefore, the requirement of a variable reactive power source is needed; STATCOM is a controller that can provide the required reactive power to the HPS and maintain the constant voltage level. This kind of problem is known as KVAR-voltage control problem (Bansal and Bhatti, 2008; Kundur et al., 1994; Hingorani et al., 2000).

STATCOM is a variable reactive power support controller, providing the required reactive power to the HPS and is used widely for its better performance than other controllers such as static VAR compensator (SVC) and thyristor controlled switch capacitor (TCSC) (Hingorani et al., 2000; Barua and Quamruzzaman, 2018a; Barua and Quamruzzaman, 2018b; Barua et al., 2021a). Sharma et al. (2010) showed a comparative study of the HPS model using SVC and STATCOM controllers. Saxena and Kumar (2014, 2016) proposed GA, ANN, and ANFIS methods based on optimization related to reactive power compensation of a decentralized HPS model with a STATCOM-PI controller.

The research aims to control the reactive power (KVAR) to improve the system's stability. For that, the IPDF-controlled STATCOM has been utilized in the studied WDHPS model for the betterment of the direction of desired results multiple soft computing techniques have been applied to choose the exact parameter's value.

Therefore, this paper makes the following contributions:

- a) Intelligent reactive power control with the help of OHS optimized STATCOM-IPDF controller.
- b) Study the isolated WDHPS model with other controllers.
- c) A comparative study of the applied algorithm for optimizing the parameters for the purpose of reactive power control.
- d) Stability analysis of the WDHPS under varying load disturbances.

2. Theoretical view of the studied hybrid model

Modern power systems comprise traditional generating systems (such as diesel and thermal) along with renewable energy-based generating systems (like PV, wind, fuel cell, etc.). With each day, the penetration levels of renewable energy sources in the power system have been increased (Barua et al., 2021b) because of its various advantages, but the concept of power systems flexibility also needs to be redefined. The HPS is a combination of an SG coupled energy generating system or IG coupled energy generating system or any other. It may be the combinations of SG-coupled diesel engine and IG-coupled wind system. The WDHPS model is discussed in this research along with its block diagram representation in Fig. 1 which includes a load and a FACTS device.

As wind turbine-based IG and loads (generally reactive in their characteristics) necessitate reactive power to operate, the only source of reactive power in the WDHPS model is the diesel engine that provides mechanical power input to the SG. Thus, it is impossible to bestow the necessary quantity of reactive power to the load and IG under the disturbances, which results in various difficulties in the studied model. The deficit/additional quantity of reactive power is catered by a FACTS controller. In this model, a STATCOM controller is deployed to deliver the necessary reactive power to the system and to meet the desired system requirements at its required conditions.

In the above described WDHPS model, when any kind of small input perturbation occurs in terms of load fluctuations and wind power disturbances, the system voltage changes, thereby losing the power system flexibility. Hence, the uncertainty on the demand side also causes uncertainty on the supply side. The system voltage response will be at its desired specifications if the reactive power of the system has been compensated properly after the disturbances. The change in system voltage in terms of reactive power may be shown in the form of (1) and is derived from the transfer function model of the WDHPS model picturized in Fig. 2.

$$\Delta U(s) = \frac{K_V}{1 + sT_V} [\Delta Q_{SG} + \Delta Q_{STATCOM} - \Delta Q_{IG} - \Delta Q_{load}] \quad (1)$$

Because of the change in terminal voltage of the WDHPS, the changes also occur in reactive power consumption and supply in the devices i.e., in IG, SG, FACTS, and load. The variation of reactive power in each system has been described below.

The variations in reactive power of the wind engine supplying the IG under constant slip (s) may be described as given in Eq. (2):

$$\Delta Q_{IG} = K_1 \Delta U(s) \quad (2)$$

where K_1 is a constant written in the form of $\left[\frac{2U(x_1+x_2)}{(R_p+R_{eq})^2 + (x_1+x_2)^2} \right]$.

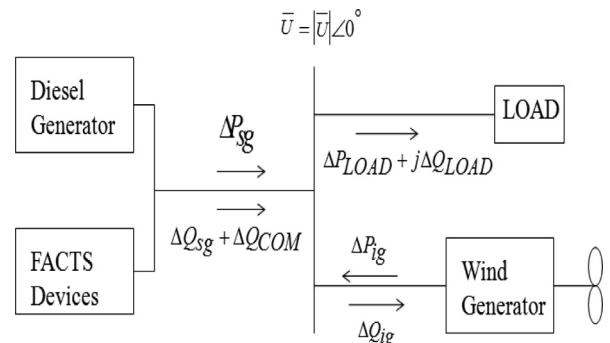


Fig. 1. Schematic of the studied isolated WDHPS model.

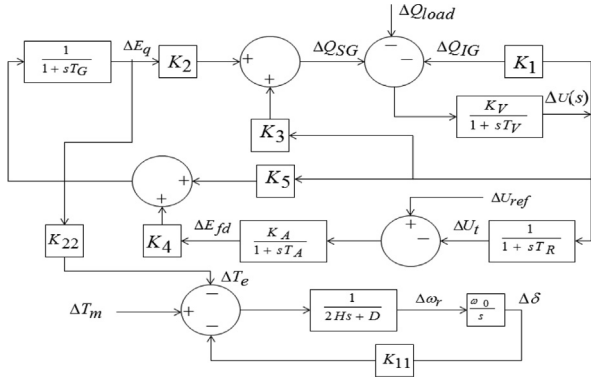


Fig. 2. WDHPS model in the Laplace domain.

In K_1 , terms R_p and R_{eq} are written as $R_p = \frac{r_2}{s}(1-s)$ and $R_{eq} = r_1 + r_2$.

The different IG parameter values (Bansal and Bhatti 2008) are $s = -35\%$, $r_1 = r_2 = 0.19p.u.$, $x_1 = x_2 = 0.56 p.u.$

The change of reactive power in diesel engine supported SG may be written as in Eq.(3).

$$\Delta Q_{SG} = K_2 \Delta E_q(s) + K_3 \Delta U(s) \quad (3)$$

In Eq. (3), the internal armature emf (ΔE_q) depends directly on the direct axis field flux under steady-state operating mode. The change in armature emf under any small perturbation may be written as (4):

$$\Delta E_q = \left(\frac{1}{1+sT_G} \right) (K_4 \Delta E_{fd}(s) + K_5 \Delta U(s)) \quad (4)$$

The constants associated with Eqs. (3) and (4) i.e., K_2 , K_3 , K_4 , and K_5 are explained in Appendix.

The reactive power deficit of the WDHPS model is fulfilled by the FACTS controller. Among the various FACTS controllers, STATCOM is more efficient to control the reactive power under any disturbances on the HPS model due to its excellent characteristics than the other FACTS devices (Kuo and Wang, 2001). The modeling of the STATCOM controller for reactive power control and stability improvement has been illustrated in the subsequent section.

2.1. Design of the controller

STATCOM is developed on the solid-state-based synchronous source of voltage which replicates a synchronous machine of ideal nature. It generates a set of 3-phase balanced sinusoidal voltages at the fundamental frequency by continuous controlling of phase angle and amplitude. The schematic of the STATCOM and its equivalent structure has been given in Fig. 3(a) and (b). Fig. 3(a) illustrates the voltage source converter, DC capacitor, and coupling transformer. The real part of the STATCOM controller current is insignificant and considered zero. The reactive current can be controlled by the variation of α and δ as given in Fig. 3(b).

In this paper, α is the STATCOM's fundamental output voltage (kU_{dc}) phase angle and δ is the phase angle of the system bus voltage, U where the STATCOM is connected (Chakrabarti and Halder, 2010; Kouadri and Tahir, 2008). The amplitude of the converter's fundamental output voltage is kU_{dc} where U_{dc} represents DC voltage developed in between the DC capacitor. The STATCOM controller injecting the reactive power to the connected bus has been given as (Kouadri and Tahir, 2008) in Eq. (5).

$$Q_{STATCOM} = kU_{dc}^2 B - kU_{dc} UB \cos(\alpha - \delta) + kU_{dc} UG \sin(\alpha - \delta) \quad (5)$$

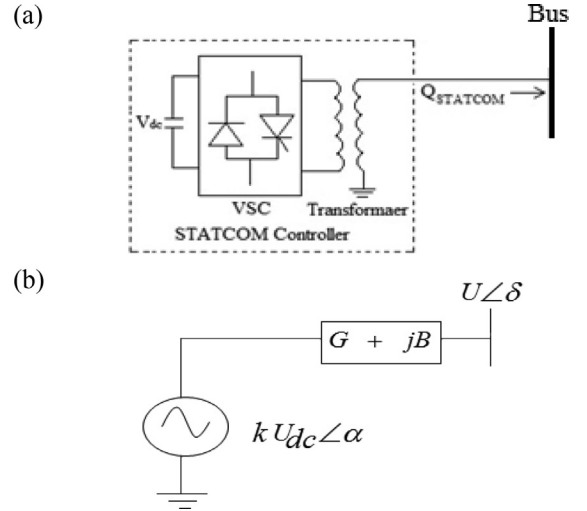


Fig. 3. STATCOM configurations (a) schematic and (b) equivalent model.

In the considered HPS, bus voltage is taken as a reference voltage; so, the bus angle (δ) is zero. In the above equation, the G term is also insignificant, because $(G + jB)$ characterizes the admittance of the step-down transformer. Thus, Eq. (5) now becomes Eq. (6), considering G and δ as zero.

$$Q_{STATCOM} = kU_{dc}^2 B - kU_{dc} UB \cos \alpha \quad (6)$$

Here, in Eq. (6), U and α , are the variable terms on which the reactive power depends; under the small perturbations, the change in reactive power of STATCOM can be written as Eq. (7).

$$\Delta Q_{STATCOM} = \frac{\partial Q_{STATCOM}}{\partial \alpha} \Delta \alpha + \frac{\partial Q_{STATCOM}}{\partial U} \Delta U \quad (7)$$

Again (7) can be written as (8):

$$\Delta Q_{STATCOM}(s) = G_1 \Delta \alpha(s) + G_2 \Delta U(s) \quad (8)$$

where $G_1 = kU_{dc} UB \sin \alpha$ and $G_2 = -kU_{dc} UB \cos \alpha$.

Taking these equations of the STATCOM controller, a simulation model in the s -domain is developed and given in Fig. 4.

3. State space modeling approach of the studied WDHPS

The state equations (Bansal and Bhatti, 2008) of the studied WDHPS can be written in the form of (9).

$$\dot{X} = [A] X + [B] M + [C] P \quad (9)$$

where the terms X , M , and P are the state, control as well as disturbance vectors, and their corresponding A , B , and C terms are the

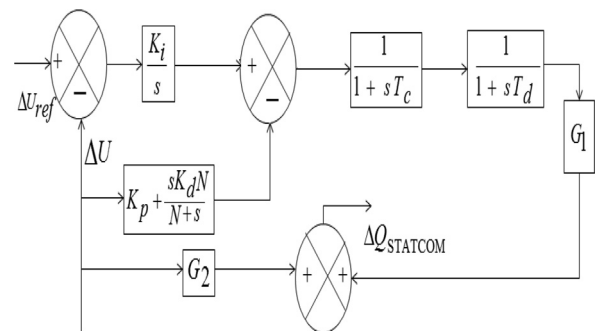


Fig. 4. Small-signal modeling of the STATCOM-IPDF.

state, control, and disturbance matrices, respectively. The transfer function of the studied WDHPS with control of reactive power has been depicted in Fig. 2, and the state space vectors of this system are given as:

Case A: Only the WDHPS model

$$\Delta \underline{X} = [\Delta\omega_r, \Delta\delta, \Delta E_{fd}, \Delta E_q, \Delta U_t, \Delta U]^T$$

$$\Delta \underline{M} = [\Delta U_{ref} \quad \Delta T_m]^T$$

$$\Delta \underline{P} = [\Delta Q_{ref}]$$

For this case of the WDHPS model, no tunable parameters are present.

Case B: WDHPS model with IPDF and STATCOM controller.

$$\Delta \underline{X} = [\Delta\omega_r, \Delta\delta, \Delta E_{fd}, \Delta E_q, \Delta U_t, \Delta U, \Delta Y_1, \Delta Y_2, \Delta \alpha]^T$$

$$\Delta \underline{M} = [\Delta U_{ref} \quad \Delta T_m]^T$$

$$\Delta \underline{P} = [\Delta Q_{ref}]$$

The tunable parameters and their ranges attached to this considered case are $-10 \leq K_p, K_i, K_d \leq 100; 10 \leq N \leq 100; 0.01 \leq T_c, T_d \leq 1.67$.

4. Problem formulation of the studied WDHPS model

The change in reactive power output of the STATCOM controller is due to variations in firing angle along with voltage. The adjustment of firing angle for reactive power compensation is done with deviation in voltage being utilized as the controller's reference signal. The fast and accurate tuning of K_p, K_i, K_d, N (derivative filter coefficient), T_c , and T_d leads to a better RPC of the WDHPS. In the case of optimizing the parameter, an effort is made to find the optimal setting of the parameters of the controller. The optimal settings of the parameters have been done by OHS, SOS, BGA, and ALO-based optimization techniques. The main motto of this optimization process is to provide adequate damping of the power system oscillations under any disturbances and is accomplished by escalating the damping ratio of the damped eigenvalues of the studied WDHPS model. The parameters are adjusted using the following criterion that is interrelated with the eigenvalues of the WDHPS. The objective function (J) (Chatterjee et al., 2009) criterion is shown in Eq. (10).

$$J = J_1 + 10J_2 + 0.01J_3 + J_4 \quad (10)$$

4.1. Measure of performance indices

The optimization of performance indices is done to augment the stability margin for the HPS which is achieved by better damping along with getting a minimum increment in case of the terminal voltage. This means the depletion of steady-state error (E_{ss}) of the terminal voltage response. The performance indices terms are considered as in Eqs. (11)–(13), (Hekimoğlu, 2019).

$$IAE = \int_0^{\infty} |U_t(t)| dt \quad (11)$$

$$ISE = \int_0^{\infty} U_t^2(t) dt \quad (12)$$

$$ISTE = \int_0^{\infty} t \times U_t^2(t) dt \quad (13)$$

5. Discussion on the applied algorithm

5.1. Harmonic search algorithm

Prompted by the natural performance of music, Geem et al. proposed *Harmonic Search Algorithm* in 2001. This algorithm converges with the constant exploration of a better state of harmony. As it is a stochastic algorithm, this method has lesser mathematical desideratum in comparison to other than most metaheuristic techniques. The solution of the algorithm works analogously with the harmony present in the music. The global and local searches are evaluated analogous to the improvisation of the musician. With the lesser necessity of input conditions, the algorithm is well adaptable for various engineering problems. For most practical engineering like structural optimization problems (Lee and Geem, 2004) HS algorithm has proven to be faster than GA (Genetic Algorithm) (Mahdavi et al., 2007). Other applications of this algorithm include estimation of parameters of the nonlinear Muskingum model (Kim et al., 2001), network design of pipes (Geem et al., 2002), routing of vehicles (Geem et al., 2005), designing of distribution networks of water (Geem, 2006), and schedule of multiple dam system (Geem, 2007). The proposed algorithm by Geem et al. has the potential of discovering good domains of solution spaces within an appropriate time span. Few modified versions of HS have also been suggested in the literature. In the case of the harmony search algorithm, every potential solution is termed harmony and is represented as an n^{th} dimensional real vector. A randomly generated set of these vectors is stored in the harmony memory (HM). With the consideration of the pitch adjustment rule, memory consideration rule as well as random re-initialization a new candidate harmony is developed. Finally, the HM is reformed after comparing the worst vector in the memory with the new vector replacing the worst one. This process is repeated until the termination criterion is satisfied.

5.2. Oppositional harmonic search

Tizhoosh has introduced the concept of the Oppositional Harmonic Search algorithm (Tizhoosh, 2005a). The concept of Opposition is applied to accelerate the convergence rate. Generally, it is used for backpropagation (Ventresca and Tizhoosh, 2006) as well as re-enforcement learning (Tizhoosh, 2005b; Tizhoosh, 2006). In the case of an oppositional harmonic search algorithm, estimates of the candidate solution and its corresponding opposite estimate are derived to have a better conjecture of the present candidate solution vector. The ideology of incorporating opposite estimates is used while initializing harmony memory and also during the development of New Harmony vectors undergoing the procedure of harmony search. In this work, the incorporation of the oppositional-based algorithm is used to enhance the convergence of the harmony search algorithm. In the case of any stochastic optimization methodology, a random initialization is performed. The rate of convergence depends on how far our initial random guess is from the optimal result. Incorporating opposite numbers, a closer estimate of the solution is achieved by testing both the solution and its opposite solution as well. With these techniques, fitter solutions (be it the primitive guess or its opposite) are adopted as the initial solution. Thus, the closer approximation as evaluated by the fitness function is used for accelerated convergence. It is used not only for an initial solution but also at each iteration.

5.3. Declaration of opposite estimates

Any random initial solution vector or real number can be termed as x and let it be bounded between lb (lower bound) and an ub (upper bound). An opposite estimate is declared as (14).

$$\bar{x} = lb + ub - x \quad (14)$$

It can be extended to higher-order dimensions of vector space (Tizhoosh, 2006).

5.4. Declaration of opposite vector space

Let $X = (x_1, x_2, x_3, \dots, x_n)$ represent an n^{th} order vector space where all components $x_1, x_2, x_3, \dots, x_n$ are components of the real number axis. Again defining: $x_i \in [ub_i, lb_i] \forall i \in \{1, 2, 3, \dots, n\}$. The opposite guess $\bar{x} = (\bar{x}_1, \bar{x}_2, \bar{x}_3, \dots, \bar{x}_n)$ is declared as (15).

$$\bar{x}_i = lb_i + ub_i - x_i \quad (15)$$

The following subsection emphasizes opposite point optimization incorporating the declaration of opposite vector space.

5.5. Opposition based optimization

Assuming $f = (\cdot)$ is the fitness function used for estimation of fitness of candidate solution, with the declaration of X and \bar{x} being the opposite estimates we inspect the fitness of these two points. If $f(\bar{x}) \leq f(X)$ the candidate solution, X can be substituted by \bar{x} ; in other cases, we sustain with X . Thus, we simultaneously evaluate the fitness of the randomly generated point and its opposite estimate to obtain the fitter one.

5.6. Opposition harmony search algorithm

Analogous to all population-based optimization methodologies there are two major steps for the HS technique. HM initialization and development of new HM is analogous to the HS algorithm. The Opposition-based algorithm is embedded within the HS algorithm so as to enhance the rate of convergence. The following pseudo-code can be adapted for the proposed algorithm.

OHS Algorithm

- Initialization of parameters, viz. HMS , $HMCR$, PAR_{min} , BW_{min} , PAR_{max} , BW_{max} as well as NI .
- Initialization of the harmony memory with a random set of initial guesses X_{0ij} .
- Harmony Memory initialization with Oppositional algorithm embedded within it

for ($i1 = 0; i1 < HMS; i1 ++$)

for ($j1 = 0; j1 < n; j1 ++$)

$$OPOX_{0i1j1} = PAR_{j1}^{min} + PAR_{j1}^{max} - X_{0i1j1}$$

end for

end for

Selection of HMS as fittest candidate solutions from the set of $\{X_{0i1j1}, OX_{0i1j1}\}$ as initial HM comprising of the fittest X vectors.

- Introduction of a new X^{new} as follows:-

for ($i1 = 0; i1 < HMS; i1 ++$)

for ($j1 = 0; j1 < n; j1 ++$)

if ($r_1 < HMCR$) then

$$X_{i1j1}^{new} = X_{i1j1}^a // a \in (1, 2, 3, \dots, HMS)$$

if ($r_2 < PAR(gn)$) then

a (continued)

OHS Algorithm

$$X_{i1j1}^{new} = X_{i1j1}^{new} \pm r_3 BW(gn) // r_1, r_2, r_3 \in [0, 1]$$

end if

else

$$X_{i1j1}^{new} = PAR_{i1j1}^{min} + r \times (PAR_{i1j1}^{max} - PAR_{i1j1}^{min}) // r \in [0, 1]$$

end if

end for

- Updating of Harmony memory is done by evaluation of the following fitness function

$$X^{worst} = X^{new} \text{ if } f(X^{new}) < f(X^{worst})$$

- Updating of Harmony memory is done by evaluation of the following fitness function

if ($rand_2 < J_r$) // $rand_2 \in [0, 1]$ and J_r is the rate of jumping

for ($i1 = 0; i1 < HMS; i1 ++$)

for ($j1 = 0; j1 < n; j1 ++$)

$$OPOX_{i1j1} = \min_{j1}^{gn} + \max_{j1}^{gn} - X_{i1j1}$$

Where \min_{j1}^{gn} represents the minimal magnitude of a j^{th} variable in the current generation of candidate solution (gn) and \max_{j1}^{gn} represents the maximum magnitude of the j^{th} variable in the current generation of candidate solution (gn)

end for

end for

end if

Selection of new HM from the fittest HMS with the aid of $[X_{ij}, OPX_{ij}]$

Termination of oppositional-based harmony search jumping.

- If NI or termination criteria are satisfied, returns the fittest harmony vector X_{best} in the HM, unless go to step d.

6. Simulation results with discussion

The simulation of the abovementioned considered isolated WDHP model was done using the MATLAB system. Simulations were worked out with two diverse cases (i.e., only the WDHP model and the WDHP model with IPDF-STATCOM controller). Various parameters of the two different test cases model are optimized by different algorithms (i.e., OHS, ALO, BGA, and SOS). The model various outcomes after the simulation with different input conditions are observed and discussed following.

6.1. Objective function-based analysis

Different parameters under Case B are given in Table 1 by applying different soft computing techniques, considering Eq. (10) as the objective function. Under the loading conditions (i.e., under constant load variation and under varying step load) the WDHP model has been examined. Table 1 shows that J has optimized at a lower value for Case B. The value is also less for the OHS-based optimizing parameters techniques. It may be concluded that the model parameters are well optimized for the OHS techniques, and hence, the considered objective function is lowered in that situation.

6.2. Superiority of the proposed algorithm on the verge of the convergence profile curve

In this section, the superiority among the applied algorithms has been discussed in view of convergence profiles. Here, the proposed OHS algorithm for designing STATCOM-IPDF is compared

Table 1
Optimal parameters and convergence value under different load disturbances for Case B: Model + STATCOM-IPDF.

Input conditions	Applied algorithms	Fitness value	Optimal parameters					
			K_p	K_i	K_d	T_c	T_d	N
Constant Load	SOS	417.0939	1.0000	10.0000	6.7225	0.0030	0.0020	10.0000
	ALO	414.0450	0.0010	10.0000	29.4636	0.4773	0.4817	55.9662
	BGA	413.8975	10.0000	99.6484	10.0000	0.0025	0.0017	10.0000
	OHS	412.5506	0.0010	40.0000	6.7890	0.0030	0.0200	10.0000
1% Load Disturbance	SOS	417.0939	1.0000	10.0000	6.7225	0.0030	0.0020	10.0000
	ALO	414.4270	0.0010	10.0000	30.2245	0.3991	0.5446	138.8370
	BGA	413.3208	68.3594	97.5391	21.9531	0.4960	0.8700	97.8906
	OHS	412.5506	0.0010	40.0000	6.7890	0.0030	0.0200	10.0000
2% Load Disturbance	SOS	417.0939	1.0000	10.0000	6.7225	0.0030	0.0020	10.0000
	ALO	414.4178	0.0010	10.0000	37.43263	0.1116621	0.6402511	188.0015
	BGA	413.4127	63.4375	84.5313	30.3906	0.7220	0.4882	93.6719
	OHS	412.5506	0.0010	40.0000	6.7890	0.0030	0.0200	10.0000
5% Load Disturbance	SOS	417.0939	1.0000	10.0000	6.7225	0.0030	0.0020	10.0000
	ALO	414.4128	0.001	10.0000	38.85418	0.6376966	0.08786283	262.3505
	BGA	413.5271	25.4688	95.0781	10.3516	0.4414	0.5038	25.4688
	OHS	412.5506	0.0010	40.0000	6.7890	0.0030	0.0200	10.0000
10% Load Disturbance	SOS	417.0939	1.0000	10.0000	6.7225	0.0030	0.0020	10.0000
	ALO	414.4397	0.001	10.0000	31.4564	0.544715	0.373214	69.0355
	BGA	413.6325	92.9688	90.8594	17.7344	0.7687	0.8700	80.6641
	OHS	412.5506	0.0010	40.0000	6.7890	0.0030	0.0200	10.0000
10% Variable Load Disturbance	SOS	417.0939	1.0000	10.0000	6.7225	0.0030	0.0020	10.0000
	ALO	416.7865	0.001001	10.0000	29.85561	0.4811049	0.476508	176.7762
	BGA	415.9436	69.4141	98.5938	30.0391	0.6908	0.4882	36.3672
	OHS	412.5506	0.0010	40.0000	6.7890	0.0030	0.0200	10.0000

with the other discussed algorithms (*i.e.*, ALO, BGA, and SOS with STATCOM). Fig. 5 shows the variations of J for four different optimization algorithms. The J decreases in each case of applied techniques though with different rates of decrease in every case. The OHS optimized J converges very fast with a lower convergence value than the others.

The number of iterations required to converge under different algorithms is given in Table 2. Table 2 and Fig. 5 show that the proposed methodology (*i.e.*, OHS technique for optimized STATCOM with the IPDF controller) is better than the others.

6.3. Response under normal loading condition

The corroboration of the WDHPs performance because of a 1% increase in mechanical torque (T_m) for the generator and the reference voltage (V_{ref}) as a minor disturbance is verified. Fig. 6 (a) and (b) show the effects on terminal voltage of the WDHPs due to 5% and 10% step load disturbance. It can be shown that the system with the suggested OHS-STATCOM is more stabilized than ALO-STATCOM, BGA-STATCOM, and SOS-STATCOM. In addition, the

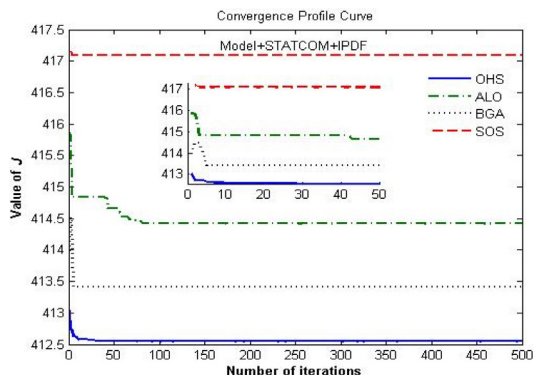


Fig. 5. Convergence profile curve under 2% load disturbance.

Table 2
Number of iterations to converge under 2% disturbances in load.

Applied algorithms	Number of iterations
SOS	5
ALO	42
BGA	8
OHS	3

required mean settling time to diminish system oscillations is roughly about 0.497 s with OHS-STATCOM and 0.72 s, 1.48 s, and 0.6 s for ALO-STATCOM, BGA-STATCOM, and SOS-STATCOM, respectively, for 5% load disturbance. On the other hand, the system with no controller has huge oscillations because of not fulfilling the reactive power of the system itself, as shown in Fig. 7.

6.4. Response under varying load conditions

The transient voltage responses of the studied WDHPs are also taken into consideration. In this study, we have considered two different types of variable loads a) step load variation and b) sudden impulse load input. The results of interest are obtained with the considered cases (*i.e.*, only the WDHPs model and WDHPs model with the IPDF-STATCOM).

6.4.1. Variable step load condition

In the studied WDHPs model, a step variable load, as shown in Fig. 8, is applied. Then, a certain input load perturbation of 10% has been considered. After the perturbation, the transient voltage responses have been given in Figs. 9 and 10, for the two considered test cases. The figures show that the STATCOM-IPDF controller has a more tremendous capability to manage the reactive power of the WDHPs than that of the other controllers. Thus, the stability of the whole system is also enhanced.

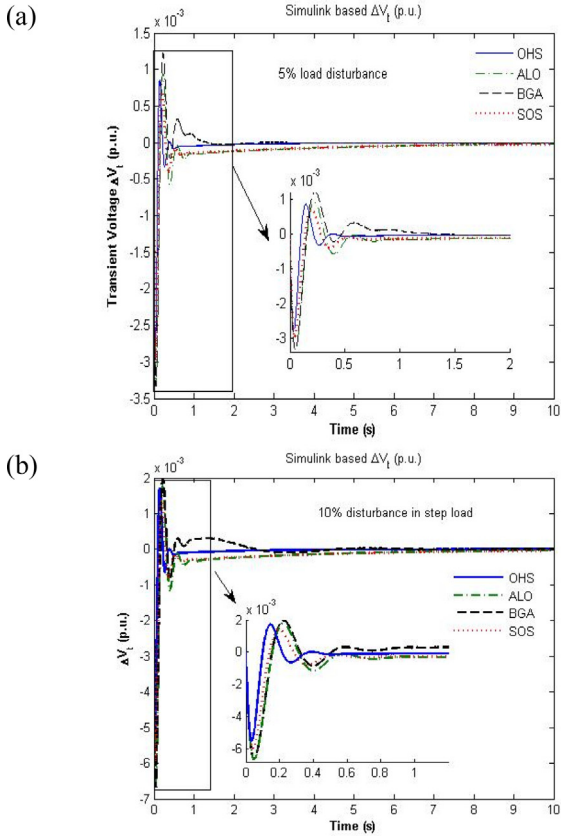


Fig. 6. Transient response under (a) 5% and (b) 10% load disturbance.

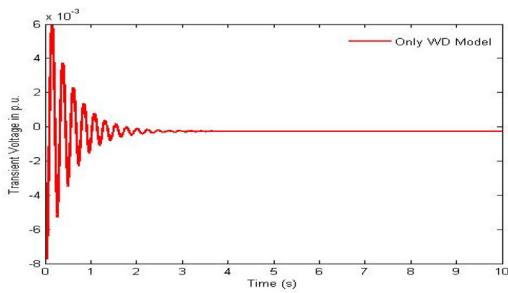


Fig. 7. Transient response of WDHPS model without any controller under 5% load input disturbance.

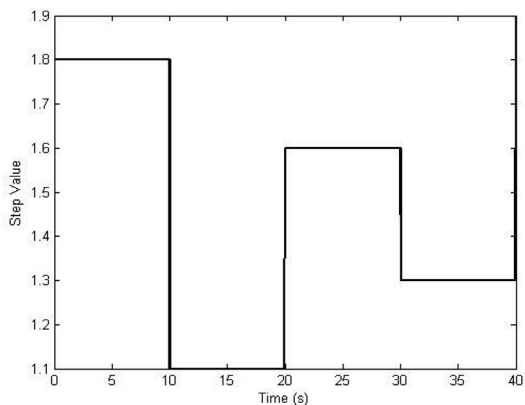


Fig. 8. Variable step load waveform.

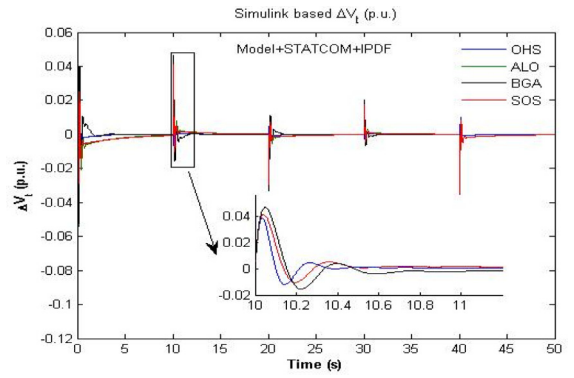


Fig. 9. Response under variable step load disturbance.

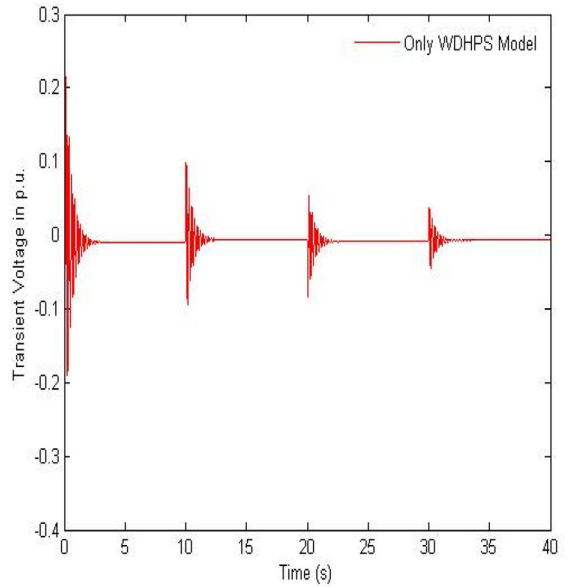


Fig. 10. Response under variable step load disturbance for only WDHPS.

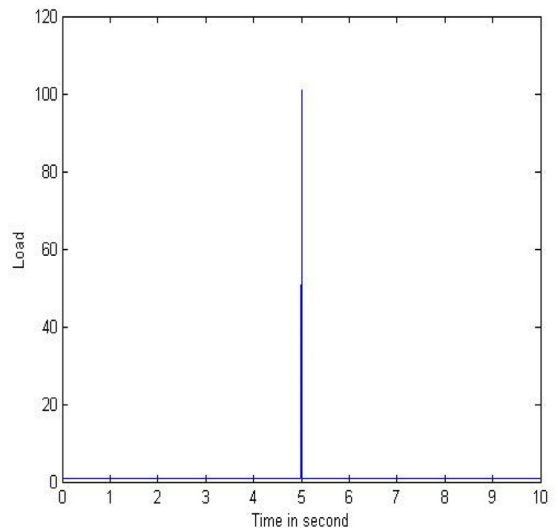


Fig. 11. Input with constant and impulse load disturbance.

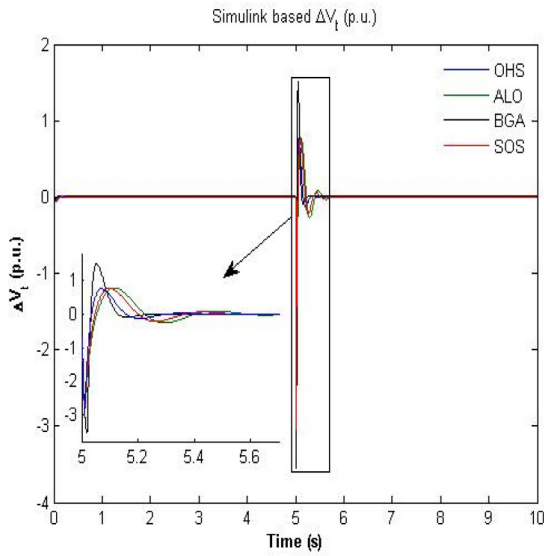


Fig. 12. Comparison of responses under impulse load disturbance.

6.4.2. Under impulse load injection

An impulse load has been injected with the constant load in the studied WDHPS model, as shown in Fig. 11. Fig. 12 clarifies that the WDHPS model under the OHS with STATCOM-IPDF condition gives better stability.

6.5. Figure of Demerit-based analysis

Another performance criterion in the time domain has been measured to assess the STATCOM-IPDF controller. A set of good control parameters (i.e., $K_p, K_i, K_d, T_c, T_d,$ and N) results in a good step response leading to minimization of performance criteria in the time domain. The set of good parameters values is determined by the SOS, ALO, BGA, and OHS algorithm techniques and compared to their results also. The time-domain performance criterion is mentioned in a way that is related to the overshoot (M_p), settling time (t_s), rise time (t_r) as well as E_{ss} . The performance criterion (i.e., $W(K)$) is defined as follows (Gaing, 2004) in (16).

$$\text{Min } [W(K)] = \text{Min } [FOD]$$

here

$$FOD = (1 - e^{-\beta}) * (M_p + E_{ss}) + e^{-\beta}(t_s - t_r) \tag{16}$$

where K is dependent on $[K_p, K_i, K_d, T_c, T_d,$ and $N]$ and β is the weighting factor.

The $W(K)$ satisfies the designer requirements using the β factor. With the weighting factor chosen >0.7 , it is observed that the M_p and E_{ss} are reduced. On the other hand, a value <0.7 shows a reduction in t_r as well as t_s (Gaing, 2004).

Table 3 Performance criterion (i.e., FOD) and other parameter values.

Load disturbance in p.u.	Applied soft computing techniques	$M_p \times 10^{-4}$	$E_{ss} \times 10^{-5}$	FOD
2%	SOS	2.7856	-1.9726	0.7666
	ALO	3.7089	-1.9378	0.7690
	BGA	4.2601	-0.27488	0.7694
	OHS	0.00000003	-0.0000	0.3273
5%	SOS	6.9725	-5.1715	0.7666
	ALO	9.3922	4.4351	0.7686
	BGA	0.00000012	-0.20111	0.7692
	OHS	0.00000009	-0.0000	0.3279

Table 4 Performances indices value under different load disturbance conditions for WDHPS model + STATCOM-IPDF.

Load disturbances in p.u.	Applied algorithms	IAE	ISE	ITSE
1%	SOS	0.7110	0.0009	0.00003
	ALO	72.3365	1.3171	0.2885
	BGA	0.6917	0.00125	0.00006
	OHS	0.2923	0.0001	0.0000
2%	SOS	1.3689	0.00036	0.00011
	ALO	1.4910	0.00052	0.00012
	BGA	0.8578	0.00049	0.00005
	OHS	0.5304	0.0002	0.0000
5%	SOS	3.3394	0.0023	0.00066
	ALO	3.6512	0.0032	0.00074
	BGA	1.9987	0.0032	0.00031
	OHS	1.2455	0.0014	0.0001
10%	SOS	6.6260	0.0091	0.0026
	ALO	7.205	0.0129	0.0029
	BGA	4.9554	0.0124	0.0015
	OHS	2.4365	0.0054	0.0004
10% Variable step load	SOS	241.9829	3.9560	4.9439
	ALO	228.6391	5.2191	4.2338
	BGA	139.0227	5.1124	4.0869
	OHS	93.1518	2.4032	2.9604

In this study, we considered 1.0 as the weighting factor value to minimize the M_p along with the E_{ss} . The minimum value of performance criterion under various applied algorithms for the WDHPS model with STATCOM-IPDF controller is given in Table 3. Table 3 shows that the performance criterion value and the M_p , as well as E_{ss} , value are minimal under the OHS optimization technique. Thus, for a certain set of K values under (2% and 5%) load disturbances, the OHS algorithm is very fruitful than other algorithms.

6.6. Performance indices analysis

The various parameters (i.e., IAE, ISE, and ITSE) values under certain load disturbances are given in Table 4. The result shows that the performance indices decrease chronologically from the use of only the WDHPS model, and lastly, the WDHPS model with STATCOM-IPDF controller. The result is also better for the OHS optimization technique.

7. Conclusion

In this study, a STATCOM-IPDF controller has been successfully implemented in the WDHPS model for reactive power compensation. The reactive power is intelligently controlled by the said controller under any kind of perturbations. With the proper control of reactive power, the WDHPS model is found to be stable, and an improvement is achieved using this controller in comparison to the earlier discussed controller in the literature. The compensation of reactive power is given better results when various soft computing techniques are applied to it for WDHPS controller parameters optimization. It also may be said that the OHS algorithm is very much fruitful for the parameter optimization than other applied algorithms. Thus, it may become a very much useful application for the stability improvement of the WDHPS model.

Authors' Contributions

All authors have equally contributed to the analysis and interpretation of the results and data, drafting the article, revising it critically and preparing the final version.

Funding

No funding has been received for this research work.

Code Availability (Software Application or Custom Code)

The custom code is available from the corresponding author on request.

Declaration of Competing Interest

The authors declare that they have no known competing financial interests or personal relationships that could have appeared to influence the work reported in this paper.

Appendix

The different constant parameters related to (3) & (4) are given as follows:

$$K_2 = \frac{U \cos \delta}{X'_d} \quad (A1)$$

$$K_3 = \frac{(E \cos \delta - 2U)}{X'_d} \quad (A2)$$

$$K_4 = \frac{X'_d}{X_d} \quad (A3)$$

$$K_5 = \frac{(X'_d - X_d) \cos \delta}{X'_d} \quad (A4)$$

$$T_G = T_{d0} \frac{X'_d}{X_d} \quad (A5)$$

The SG parameters value (Bansal and Bhatti, 2008) are considered as $U = 1.0$ p.u., $\delta = 17.2483^\circ$, $T'_{d0} = 0.05$ s, $X_d = 1.0$ p.u. and $X'_d = 0.15$ p.u.

The other data of the proposed IPDF controlled STATCOM based WDHPs model are considered as (Bansal and Bhatti, 2008; Saxena and Kumar, 2016):

$P_{IG} = 0.6$ p.u.kW, $Q_{IG} = 0.291$ p.u.kVAr, $P_{in} = 0.667$ p.u.kW, $\eta = 90\%$, p.f. in IG = 0.9, $P_{load} = 1.0$ p.u.kW, $Q_{load} = 0.75$ p.u.kVAr, p.f. of load = 0.8, $P_{SG} = 0.4$ p.u.kW, $Q_{SG} = 0.2$ p.u.kVAr, $E_q = 1.12418$ p.u., $E'_q = 0.9804$ p.u., $Q_{STATCOM} = 0.841$ p.u.kVAr and $\alpha = 53.32^\circ$.

Other considered constant parameters of the model shown in Fig. 2 are as follows:

$K_A = 200$, $T_A = 0.05$, $T_R = 0.02$, $G_1 = 1.478$, $G_2 = 3.8347$, $K_V = 0.667$, $T_V = 7.855 \times 10^{-4}$, $H = 1.0$, $D = 0.8$ and $\omega_0 = 314$.

References

- Ali, E.S., Abd Elazim, S.M., Abdelaziz, A.Y., 2017. Ant Lion Optimization Algorithm for optimal location and sizing of renewable distributed generations. *Renewable Energy* 101, 1311–1324.
- Altbawi, S.M.A., Mokhtar, A.S.B., Jumani, T.A., Khan, I., Hamadneh, N.N., Khan, A., 2021. Optimal design of Fractional order PID controller based Automatic voltage regulator system using gradient-based optimization algorithm. *J. King Saud Univ. Eng. Sci.* <https://doi.org/10.1016/j.jksues.2021.07.009>.
- Arya, Y., 2019. Impact of hydrogen aqua electrolyzer-fuel cell units on automatic generation control of power systems with a new optimal fuzzy TIDF-II controller. *Renewable Energy* 139, 468–482.
- Barua, P., Quamruzzaman, M., 2018a. Comparison between TCSC, SVC and TCSC, STATCOM based compensation on East-West interconnectors of Bangladesh power system. In: Proceedings of the 4th International Conference on Electrical Engineering and Information & Communication Technology iCEEICT 2018, Dhaka, Bangladesh, 5–8.

- Barua, P., Quamruzzaman, M., 2018b. Steady state voltage vulnerability and stability limit analysis of Bangladesh power system using STATCOM as a shunt compensator. In: Proceedings of the 4th International Conference on Electrical Engineering and Information & Communication Technology iCEEICT 2018, Dhaka, Bangladesh, 1–4.
- Barua, P., Barua, R., Quamruzzaman, M., Rabbani, M.G., 2021a. Small signal stability and transient stability improvement of Bangladesh power system using TCSC, SVC and TCSC, STATCOM based series shunt compensator. In: Proceedings of the International Conference on Science & Contemporary Technologies ICSC 2021, Dhaka, Bangladesh, 1–5.
- Barua, P., Barua, R., Quamruzzaman, M., Rabbani, M.G., 2021b. Influence of large scale solar power on stability of east west interconnector system of Bangladesh power system. In: Proceedings of the 5th International Conference on Electrical Engineering and Information & Communication Technology iCEEICT 2021, Dhaka, Bangladesh, 1–4.
- Bansal, R.C., Bhatti, T.S., 2008. *Small Signal Analysis of Isolated Hybrid Power Systems: Reactive Power and Frequency Control Analysis*. Narosa Publishers, New Delhi.
- Chakrabarti, A., Halder, S., 2010. *Power System Analysis: Operation and Control*. PHI Learning Pvt. Ltd., New Delhi, p. 3.
- Chatterjee, A., Mukherjee, V., Ghoshal, S.P., 2009. Velocity relaxed and craziness-based swarm optimized intelligent PID and PSS controlled AVR system. *Int. J. Electr. Power Energy Syst.* 31 (7–8), 323–333.
- Dai, C., Chen, W., Zhu, Y., Zhang, X., 2009. Seeker optimization algorithm for optimal reactive power dispatch. *IEEE Trans. Power Syst.* 24 (3), 1218–1223.
- Gaing, Z.-L., 2004. A particle swarm optimization approach for optimum design of PID controller in AVR system. *IEEE Trans. Energy Convers.* 19 (2), 384–391.
- Geem, Z.W., Kim, J.H., Loganathan, G.V., 2001. A new heuristic optimization algorithm: harmony search. *Simulation* 76 (2), 60–68.
- Geem, Z.W., Kim, J.H., Loganathan, G.V., 2002. Harmony search optimization: application to pipe network design. *Int. J. Model. Simul.* 22 (2), 125–133.
- Geem, Z.W., Lee, K.S., Park, Y., 2005. Application of harmony search to vehicle routing. *Am. J. Appl. Sci.* 2 (12), 1552–1557.
- Geem, Z.W., 2006. Optimal cost design of water distribution networks using harmony search. *Eng. Optim.* 38 (3), 259–277.
- Geem, Z.W., 2007. *Optimal scheduling of multiple dam system using harmony search algorithm*. Lecture Notes in Computer Science, Springer, Berlin, Heidelberg 4507, 316–323.
- Haridoss, R., Punniyakodi, S., 2019. Compression and enhancement of medical images using opposition based harmony search algorithm. *J. Inf. Process. Syst.* 15 (2), 288–304.
- Hasanien, H.M., El-Fergany, A.A., 2016. Symbiotic organisms search algorithm for automatic generation control of interconnected power systems including wind farms. *IET Gener. Transm. Distrib.* 11 (7), 1692–1700.
- Hekimoğlu, B., 2019. Sine-cosine algorithm-based optimization for automatic voltage regulator system. *Trans. Inst. Meas. Control* 41 (6), 1761–1771.
- Hingorani, N.G., Gyugyi, L., El-Hawary, M., 2000. *Understanding FACTS: Concepts And Technology of Flexible AC Transmission Systems*. IEEE Press, New York, p. 1.
- Kim, J.H., Geem, Z.W., Kim, E.S., 2001. Parameter estimation of the nonlinear Muskingum model using harmony search. *JAWRA J. Am. Water Resour. Assoc.* 37 (5), 1131–1138.
- Kothari, D.P., 2012. Power system optimization. In: Proceedings of the second national conference on computational intelligence and signal processing CISP 2012, Guwahati, India, 18–21.
- Kouadri, B., Tahir, Y., 2008. Power flow and transient stability modeling of a 12-pulse STATCOM. *J. Cybern. Inf.* 7, 9–25.
- Kundur, P., Balu, N.J., Lauby, M.G., 1994. *Power System Stability and Control*. McGraw-hill, New York, p. 7.
- Kuo, S.C., Wang, L., 2001. Analysis of voltage control for a self-excited induction generator using a current-controlled voltage source inverter (CC-VSI). *IEE Proc. Gener. Transm. Distrib.* 148 (5), 431–438.
- Lee, K.S., Geem, Z.W., 2004. A new structural optimization method based on the harmony search algorithm. *Comput. Struct.* 82 (9–10), 781–798.
- Lurie, B.J., 1994. Three-parameter tunable tilt-integral-derivative (TID) controller. *Mahdavi, M., Fesanghary, M., Damangir, E., 2007. An improved harmony search algorithm for solving optimization problems. Appl. Math. Comput.* 188 (2), 1567–1579.
- Merrikh-Bayat, F., 2017. A uniform LMI formulation for tuning PID, multi-term fractional-order PID, and Tilt-Integral-Derivative (TID) for integer and fractional-order processes. *ISA Trans.* 68, 99–108.
- Morsali, J., Zare, K., Tarafdar Hagh, M., 2017. MGSO optimised TID-based GCSC damping controller in coordination with AGC for diverse-GENCOS multi-DISCOs power system with considering GDB and GRC non-linearity effects. *IET Gener. Transm. Distrib.* 11 (1), 193–208.
- Morsali, J., Zare, K., Tarafdar Hagh, M., 2018. A novel dynamic model and control approach for SSSC to contribute effectively in AGC of a deregulated power system. *Int. J. Electr. Power Energy Syst.* 95, 239–253.
- Patel, S., Mohanty, B., Hasanien, H.M., 2020. Competition over resources optimized fuzzy TIDF controller for frequency stabilization of hybrid micro-grid system. *Int. Trans. Electr. Energy Syst.* 30 (9). <https://doi.org/10.1002/etep.v30.910.1002/2050-7038.12513>.
- Rajinikanth, V., Latha, K., 2012. I-PD controller tuning for unstable system using bacteria foraging algorithm: a study based on various error criterion. *Appl. Comput. Intell. Soft Comput.* 2012, 1–10.

- Sahu, P.C., Prusty, R.C., Panda, S., 2020. Approaching hybridized GWO-SCA based type-II fuzzy controller in AGC of diverse energy source multi area power system. *J. King Saud Univ. Eng. Sci.* 32 (3), 186–197.
- Kumar Sahu, R., Panda, S., Biswal, A., Chandra Sekhar, G.T., 2016. Design and analysis of tilt integral derivative controller with filter for load frequency control of multi-area interconnected power systems. *ISA Trans.* 61, 251–264.
- Sahu, R.K., Sekhar, G.T.C., Priyadarshani, S., 2021. Differential evolution algorithm tuned tilt integral derivative controller with filter controller for automatic generation control. *Evol. Intel.* 14 (1), 5–20.
- Saikia, L.C., Nanda, J., Mishra, S., 2011. Performance comparison of several classical controllers in AGC for multi-area interconnected thermal system. *Int. J. Electr. Power Energy Syst.* 33 (3), 394–401.
- Sain, D., Swain, S.K., Mishra, S.K., 2016. TID and I-TD controller design for magnetic levitation system using genetic algorithm. *Perspect. Sci.* 8, 370–373.
- Sain, D., Swain, S.K., Mishra, S.K., 2018. Real time implementation of optimized I-PD controller for the magnetic levitation system using Jaya algorithm. *IFAC-PapersOnLine* 51 (1), 106–111.
- Saxena, N., Kumar, A., 2014. Reactive power compensation of an isolated hybrid power system with load interaction using ANFIS tuned STATCOM. *Front. Energy* 8 (2), 261–268.
- Saxena, N.K., Kumar, A., 2016. Reactive power control in decentralized hybrid power system with STATCOM using GA, ANN and ANFIS methods. *Int. J. Electr. Power Energy Syst.* 83, 175–187.
- Sharma, P., Kumar Saxena, N., Ramakrishna, K.S.S., Bhatti, T.S., 2010. Reactive power compensation of isolated wind-diesel hybrid power systems with STATCOM and SVC. *Int. J. Electr. Eng. Inf.* 2 (3), 192–203.
- Singh, K., Amir, M., Ahmad, F., Khan, M.A., 2021. An integral tilt derivative control strategy for frequency control in multimicrogrid system. *IEEE Syst. J.* 15 (1), 1477–1488.
- Tizhoosh, H.R., 2005a. Opposition-based learning: a new scheme for machine intelligence. In: *Proceedings of the international conference on computational intelligence for modelling, control and automation and international conference on intelligent agents, web technologies and internet commerce CIMCA-IAWTIC'06 2005*, Vienna, Austria, 1, 695–701.
- Tizhoosh, H.R., 2005b. Reinforcement learning based on actions and opposite actions. In: *Proceedings of the International Conference on Artificial Intelligence and Machine Learning AIML 2005*, Cairo, Egypt, 414, 1–5.
- Tizhoosh, H.R., 2006. Opposition-based reinforcement learning. *J. Adv. Comput. Intell. Intell. Inf.* 10 (4), 578–585.
- Ventresca, M., Tizhoosh, H.R., 2006. Improving the convergence of backpropagation by opposite transfer functions. In: *Proceedings of the IEEE International Joint Conference on Neural Network Proceedings 2006*, pp. 4777–4784.